



HAL
open science

Second-harmonic generation in sodium and niobium borophosphate glasses after poling under field-assisted silver ions anodic injection

Artem Malakho, Evelyne Fargin, Aurélien Delestre, Clément André, Thierry Cardinal, Michel Lahaye, Vincent Rodriguez, Michel Couzi, Frédéric Adamietz, Lionel Canioni, et al.

► To cite this version:

Artem Malakho, Evelyne Fargin, Aurélien Delestre, Clément André, Thierry Cardinal, et al.. Second-harmonic generation in sodium and niobium borophosphate glasses after poling under field-assisted silver ions anodic injection. *Journal of Applied Physics*, 2008, 104 (5), 053114 (4 p.). 10.1063/1.2973156 . hal-00326042

HAL Id: hal-00326042

<https://hal.science/hal-00326042>

Submitted on 4 Mar 2024

HAL is a multi-disciplinary open access archive for the deposit and dissemination of scientific research documents, whether they are published or not. The documents may come from teaching and research institutions in France or abroad, or from public or private research centers.

L'archive ouverte pluridisciplinaire **HAL**, est destinée au dépôt et à la diffusion de documents scientifiques de niveau recherche, publiés ou non, émanant des établissements d'enseignement et de recherche français ou étrangers, des laboratoires publics ou privés.



Second-harmonic generation in sodium and niobium borophosphate glasses after poling under field-assisted silver ions anodic injection

Artem Malakho, Evelyne Fargin, Aurélien Delestre, Clément André, Thierry Cardinal, Michel Lahaye, Vincent Rodriguez, Michel Couzi, Frédéric Adamietz, Lionel Canioni, and Arnaud Royon

Citation: *Journal of Applied Physics* **104**, 053114 (2008); doi: 10.1063/1.2973156

View online: <http://dx.doi.org/10.1063/1.2973156>

View Table of Contents: <http://scitation.aip.org/content/aip/journal/jap/104/5?ver=pdfcov>

Published by the [AIP Publishing](#)

Articles you may be interested in

[Towards second-harmonic generation micropatterning of glass surface](#)

Appl. Phys. Lett. **96**, 091908 (2010); 10.1063/1.3350895

[Second-harmonic generation of thermally poled silver doped sodo-borophosphate glasses](#)

J. Appl. Phys. **105**, 023105 (2009); 10.1063/1.3054182

[Stabilization of the second-order susceptibility induced in a sulfide chalcogenide glass by thermal poling](#)

J. Appl. Phys. **101**, 084905 (2007); 10.1063/1.2719008

[Poling-induced crystallization of tetragonal BaTiO₃ and enhancement of optical second-harmonic intensity in BaO–TiO₂–TeO₂ glass system](#)

Appl. Phys. Lett. **75**, 3399 (1999); 10.1063/1.125306

[Second-harmonic generation in germanosilicate glass poled with ArF laser irradiation](#)

Appl. Phys. Lett. **71**, 1032 (1997); 10.1063/1.119718



INNOVATION LEADERSHIP RELIABILITY

VALVES

GLOBAL LEADER

MODULES

CONCEPT TO PRODUCT

BELLOWS

LEADING TECHNOLOGY

SERVICES

24/7 GLOBAL SUPPORT

VAT Booth #731

APS March Meeting, Baltimore, MD

www.vatvalve.com

Second-harmonic generation in sodium and niobium borophosphate glasses after poling under field-assisted silver ions anodic injection

Artem Malakho,¹ Evelyne Fargin,^{2,a)} Aurélien Delestre,² Clément André,² Thierry Cardinal,² Michel Lahaye,² Vincent Rodriguez,³ Michel Couzi,³ Frédéric Adamietz,³ Lionel Canioni,⁴ and Arnaud Royon⁴

¹Moscow State University, Vorob'evy gory, Moscow 119991, Russia

²Institut de Chimie de la Matière Condensée de Bordeaux-UPR 9048 CNRS Université Bordeaux 1, Avenue du Dr. Schweitzer, 33608 Pessac Cedex, France

³Institut des Sciences Moléculaires, UMR 5255 CNRS, Université Bordeaux 1, 351 cours de la Libération, 33405 Talence Cedex, France

⁴Centre de Physique Moléculaire et Hertzienne, UMR 5798 CNRS, Université Bordeaux 1, 351 cours de La Libération, 33405 Talence Cedex, France

(Received 26 April 2008; accepted 23 June 2008; published online 9 September 2008)

Monovalent silver ions, resulting from a thin silver layer initially deposited at the anode surface, have been introduced using the field-assisted ion-exchange technique in sodium niobium borophosphate glasses. A reproducible susceptibility $\chi^{(2)}$ could be gained after this poling treatment, although a drop in the nonlinearity is observed due to the introduction of silver ions. From energy dispersive x-ray spectroscopy, it has been found that the nonlinear layer is characterized by a strong migration of sodium ions 4 μm deep inside the anode side, which have been partially replaced by silver ions. These results indicate a complex space-charge-migration process during the poling treatment, which is involved in the decrease in the mean second-harmonic generation signal.

© 2008 American Institute of Physics. [DOI: 10.1063/1.2973156]

I. INTRODUCTION

The development of optical communication technologies has created an important interest in materials with nonlinear optical (NLO) properties. The ideal material would combine a large nonlinear coefficient and a good optical quality with low optical losses, and also would be easy to fabricate at low costs. It is now well known that in glasses, a thermal poling treatment may induce a second-order response suitable for electro-optical applications. Myers and co-workers^{1,2} proposed a model where the second-harmonic generation (SHG) signal induced by the thermal poling process may originate either from a third-order nonlinear process through the remaining internal electric field E_{int} efficient in a layer of a few micrometers under the surface in contact with the anode, or from the extent of a structural reorganization of hyperpolarisable entities. Promising results have already been obtained for a sodium borophosphate niobium glass.^{3,4} Previously, it was reported that the doping of a silica glass surface with lithium and sodium salts results in a significant decrease in the SHG signal after thermal poling resulting from the sodium and lithium cations injection in the glass.⁵ The goal of this work is to study the influence of the silver ions injection at the anode under thermal poling.

II. EXPERIMENTS

Bulk samples with composition $0.55(0.95 \times \text{NaPO}_3 + 0.05 \times \text{Na}_2\text{B}_4\text{O}_7) + 0.45 \times \text{Nb}_2\text{O}_5$ (called BPN45 samples hereafter) were elaborated using a classical melting process.

All the characterizations presented here have been carried out on samples originating from the same batch. High purity reagent powders of NaPO_3 , $\text{Na}_2\text{B}_4\text{O}_7$, and Nb_2O_5 were mixed and grounded, poured in a platinum crucible, and melted at a temperature of 1300 °C. The melt was quenched in a brass mold (1 mm depth). The glass formed was annealed under air 30 °C under the glass transition temperature. Transparent samples with good optical quality and with surface of $\sim 1 \text{ cm}^2$ and thickness of 500 μm were cut and polished on both sides.

A square mask of silver metal resin of $\sim 0.5 \text{ cm}^2$ and with a thickness of 25 μm was sputtered on the top face (anode side) of a BPN45 glass. The thickness of the layer measured by a profilometer Tencor was found to be $\sim 180 \text{ nm}$. The glass (BPN45/Ag), being sandwiched between two electrodes with the silver resin under the anode, was then submitted to a field-assisted injection of silver during the poling treatment (1 h at 230 °C, 1 kV). The silver ions formed at the anode during the poling treatment migrated inside the glass. During the poling, the current has been recorded (Fig. 1) until the end of the ions migration when the current reached a plateau. After removing the electrodes, the anodic face of the glasses was completely transparent indicating that silver had completely been introduced inside the glass. In Fig. 1 is also reported, for the purpose of comparison, the poling current registered in the same conditions of voltage and temperature for the same glass composition without the silver thin film (BPN45). The plateau reached at long time in the current curves of both samples BPN45 and BPN45/Ag is the same.

The Raman spectra of BPN45/Ag were recorded with a Labram confocal micro-Raman instrument (Horiba/Jobin-

^{a)}Author to whom correspondence should be addressed. Electronic mail: fargin@cmcb.cnrs-bordeaux.fr.

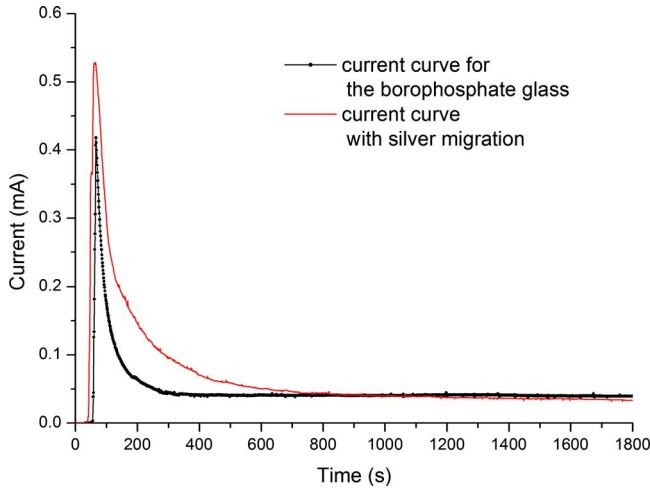


FIG. 1. (Color online) Electrical current as a function of the temperature during the field-assisted introduction of silver ions in BPN45/Ag. The same curve obtained with BPN45 is reported.

Yvon) (typical resolution of 2 cm^{-1}) in a backscattering geometry at room temperature. The spectrophotometer includes a holographic notch filter for Rayleigh rejection, a microscope equipped with a $100\times$ objective objective, and a charge coupled device (CCD) detector. The 514.5 nm emission line of an argon ion laser was used for excitation. The spectra were recorded in different zones on the poled glass (Fig. 2).

Energy dispersive x-ray spectroscopy (EDS) allowed the identification of the elemental composition of the studied samples imaged with a scanning electron microscope. The stoichiometry of the unpoled glass was first controlled. After poling, concentration profiles of silver, phosphorus, niobium, and sodium ions along the cross section of the poled glass from the anodic surface to the bulk and inside the poled region were computed (Fig. 3). The quantity of silver, which was introduced by field-assisted ion-exchange, is equivalent to the quantity of silver deposited on the surface of the glass.

Transmission spectra in the UV-visible region have been

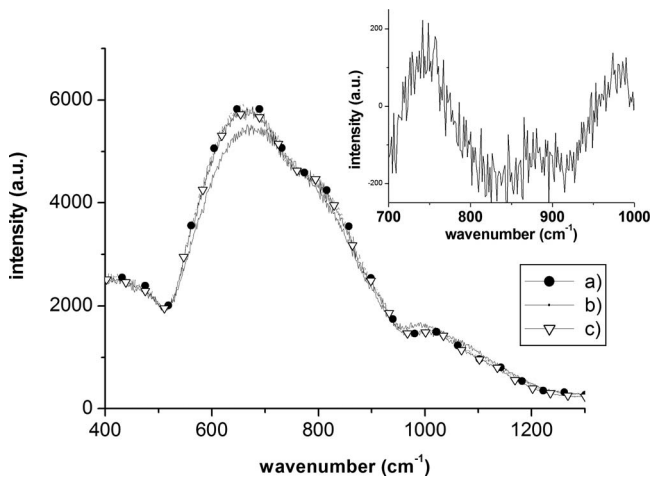


FIG. 2. Confocal micro-Raman spectra of poled BPN45/Ag: (a) at the cathodic surface, (b) at the anodic surface, and (c) $4 \mu\text{m}$ under the anodic surface. Inset is the difference spectra obtained by subtracting the normalized spectra collected in the NLO layer (b) and in the bulk of the glass (c).

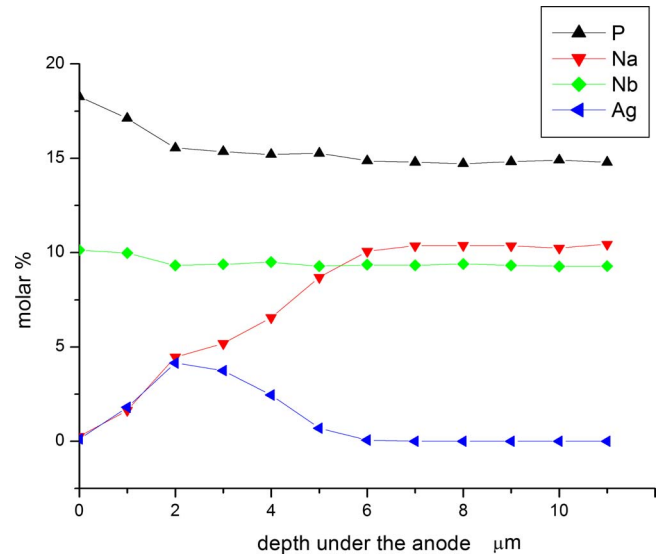


FIG. 3. (Color online) Percent atomic profiles of sodium, silver, phosphorus, and niobium ions under the anode after poling, measured by quantitative EDS.

recorded before and after poling and no difference could be evidenced. The sample, with a thickness of 1 mm, is transparent from 2500 nm, in the near infrared (IR) region, to the cutoff wavelength at 345 nm.

SHG measurements in transmission were performed on the poled sample using a 1064 nm Nd:YAG (yttrium aluminum garnet) laser line. A typical energy of $150 \mu\text{J}$ was necessary to record the transmitted *pp*- and *sp*-polarized maker-fringe patterns (Fig. 4). Details about the experimental setup are given elsewhere.⁶ In addition, the linear optical constants at 1064 and 532 nm were determined using the Brewster angle linear reflection method over the $\pm [10^\circ; 80^\circ]$ wide θ (angle of incidence) range. For poled glasses probed far enough from resonance, the contracted 3×6 SHG tensor contains two nonzero coefficients: $\chi_{33}^{(2)} = 2d_{33}$ and $\chi_{33}^{(2)} = 2d_{31}$. Since the harmonic optical response is mostly due to the interaction of the third-order susceptibility $\chi^{(3)}$ and the inter-

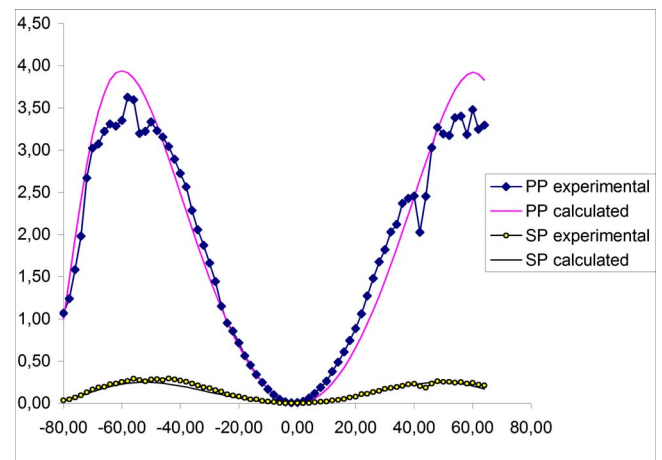


FIG. 4. (Color online) Experimental (crosses) and calculated (solid lines) transmitted polarized maker-fringe patterns of poled BPN45/Ag glass. The polarized geometries *pp* and *sp* correspond to either a *p* (in plane) or *s* (out of plane) polarized incident beam, respectively, and a *p* polarized harmonic signal.

TABLE I. Comparative results for BPN45/Ag and BPN45 samples.

	n (1064 nm \pm 0.01)	n (532 nm \pm 0.01)	$\chi^{(2)}$ (pm/V) \pm 0.1	L (μ m) \pm 0.1
Glass composition with field-assisted silver ions (BPN45/Ag)	1.91	1.94	1.2 (1 kV, 230 °C)	3.7
Glass composition without silver ^a (BPN45)	1.86	1.93	2.1 (1.25 kV, 230 °C)	3.4

^aReference 4.

nal electric field E_{int} induced by the poling treatment (1–4) [$\chi^{(2)}=3\chi^{(3)}E_{\text{int}}$], a unique component remains since $d_{33}=3d_{31}$. Following a procedure described elsewhere⁶ for the theoretical maker-fringes patterns, the NLO layer was assumed to be at the anode interface.^{3,4} Thus, two homogeneous layers have been considered with constant $d_{33}(z)$ profiles, the first layer being NLO active ($d_{33} \neq 0$) and the second one, for the remaining glass bulk, being NLO inactive ($d_{33}=0$). All the results (refractive indices, nonlinear coefficients, and nonlinear layer depths) are gathered in Table I and the corresponding simulated SHG patterns are reported in Fig. 4.

The poled glass was studied using the third-harmonic generation (THG) microscopy. This experimental setup⁷ was designed using a Zeiss axiovert 200 M microscope modified for multiphoton microscopy. Near-IR laser pulses (T -pulse laser source delivering 200 fs pulses \sim 1030 nm at a repetition rate of 50 MHz with an average power of 1.1 W) were injected into the microscope and transmitted THG signals at 343 nm were collected. Two scanning mirrors stirred the focal point of the laser in the x - y plane of the sample. The beam was focused with a 0.5 NA microscope objective at the vicinity of the glass-to-air interface, which was the anodic face, leading to a 2 μ m transverse resolution and a 5 μ m longitudinal resolution.

A x - z (x radial coordinate, z longitudinal coordinate) scan was performed across this area from the poled to the unpoled zones. A surface area of $700 \times 60 \mu\text{m}^2$ could then be imaged with either linear or circular incident polarizations. The average of the maximum values obtained from the different sample positions and from the two different polarizations is given in Table II. These values were obtained when the focus of the beam was exactly at the interface. A x - z THG image of the glass, with incident linear polarization, is reported in Fig. 5.

TABLE II. THG measurements of poled and unpoled areas with linear and circular incident polarizations at the anodic interface of BPN45/Ag after poling. The BPN45 poled glass in the same conditions was simultaneously measured for comparison and showed identical results. These nonlinear efficiencies have been recently confirmed by THG measurements using near-IR laser pulses (laser source delivering 130 fs pulses \sim 1500 nm at a repetition rate of 80 MHz) validating that corrections due to UV absorption in the glasses can be here neglected.

Polarization of the laser beam	THG signal (a.u.)	Analyzed anodic zone
Linear	$34\,000 \pm 3000$	Unpoled zone
	$43\,000 \pm 3000$	Poled zone
Circular	800 ± 1000	Unpoled zone
	$12\,000 \pm 1000$	Poled zone

III. RESULTS AND DISCUSSION

The Raman spectra exhibit slight structural differences in the NLO layer (poled area) at the anode, which disappears beyond 4 μ m. The broad and intense band at 500–1000 cm^{-1} is usually attributed to Nb–O bonds in the glass,^{4,8,9} and the evolution of its fingerprint with niobium concentration has been successfully correlated with the increase in the third-order NLO susceptibility. This band is globally affected in the poled zone, and the present features in the difference spectrum have already been observed in BPN45 poled glass without silver ions anodic injection.¹⁰

The EDS quantitative study of the P, Nb, Na, and Ag elements on the cross-section of the glass in the poled region shows the expected results. A strong depletion of sodium under the anode surface is observed until the bulk concentration is recovered 4–6 μ m under the surface (the spatial resolution being around 1 μ m for this measurement). Between the anode surface and the end of the Na^+ depleted layer, a Gaussian-like concentration profile of silver ions is observed, which has previously been called “pile-up” phenomenon.¹¹ This result is in good agreement with the qualitative differences observed in the poling current curves of BPN45 and BPN45/Ag glasses. The plateau reached at long time in the current curves of both samples is the same. However, the total charge obtained by the integration of the curve above the plateau, which corresponds to the migration of the ions, is about two times larger in BPN45/Ag, where the migration of silver ions occurs in addition to the sodium migration. Besides, the concentration profile of silver ions in BPN45/Ag is not in agreement with the theoretical concentration profile of silver, which was proposed by Lipovskii and Zhurikhina¹² for the field-assisted ion-exchange in silica glasses. This discrepancy may be explained by the high ionic conductivity of our glass due to the large concentration of sodium, but it should also be due to the different processes of silver doping. Lipovskii and Zhurikhina¹² presented the silver profile resulting from the field induced drift of ions from an unlimited source (salt melt). In the presented experiment the drift comes from a limited source (the silver thin film) accompanied by other processes such as the formation of the sodium

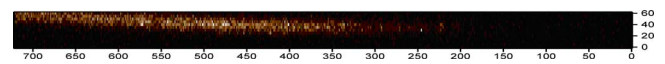


FIG. 5. (Color online) THG x - z image of the poled layer around the anode with incident linear polarization obtained in transmission along a 700 μ m line (x -axis) on the glass surface and through a 60 μ m deep zone under the anode (z -axis). The bright pixels reveal larger THG signals delivered by the poled region (the image of the poled region is not perfectly aligned due to a slight tilt of the sample with the laser beam direction).

depleted region. The silver distribution is here observed after the film dissolution giving this particular buried silver profile.

It is noticeable (see Table I) that thermal poling induces an efficient nonlinear response ($d_{33}=1.2$ pm/V) in a layer with a thickness of ~ 4 μm at the anode side, which is in agreement with the atomic modifications observed by the EDS analysis. The simulated thickness is supposed to be accurate in considering the dispersion of this glass sample and the coherence length which is quite low (~ 4.5 μm). As a consequence, we would like to point out that any etching method here is somewhat useless, in contrast to the poled silica glass exhibiting a very weak dispersion with a coherence length of ~ 20 μm and for which this method is very efficient to solve properly the question of the thickness of the NLO layer.

On one hand, this result in BPN glasses has previously been explained by a large ionic conductivity¹³ and the occurrence of a depleted layer in sodium at the anode after poling. These two conditions contribute to the stabilization of a static electric field in the glass above the anode surface. This must be combined with a large $\chi^{(3)}$ response correlated with the content of niobium in the glass.^{3,4} On the other hand, the accumulation of silver ions inside the depleted zone does contribute here to reduce the global signal from ~ 2 pm/V for BPN45 (Ref. 4) to ~ 1 pm/V for BPN45/Ag in reducing the internal field E_{int} resulting from the sodium ions migration inside the depleted zone.

The final point concerns the results obtained using the THG microscopy. For comparison purposes the THG signal was acquired for the same glass composition (BPN45) poled in the same conditions of voltage and temperature without the silver thin film deposited on the anode surface. First, a large enhancement of the THG signal with an incident linear polarization was observed in the poled zone for both glasses BPN45 and BPN45/Ag when compared to the unpoled zone. Around 20% of variation between the THG signal intensities inside and outside the poled layer was observed. This phenomenon was already described for poled BPN40 glass with $0.60(0.95 \times \text{NaPO}_3 + 0.05 \times \text{Na}_2\text{B}_4\text{O}_7) + 0.40 \times \text{Nb}_2\text{O}_5$ composition.¹⁴ The intensity of the measured THG signals is the same for both glasses within the experimental errors. This is in contradiction to the expected increase in $\chi^{(3)}$ in poled BPN45/Ag due to the presence of injected silver ions, which are more polarizable compared to sodium ions. Besides, the results in circular polarization in both glasses unambiguously show a net signal in the poled layer, indicating that the isotropy of the glass is locally broken, allowing SHG signals. Additionally, a THG in-depth study had confirmed an approximate NLO layer width around a few micrometers (the in-depth resolution was not better than 5 μm), and the collected signals at the transverse resolution scale indicated the good homogeneity of the poled glass region. However, below this resolution, it is more than likely that nonuniform

electric field distribution and concentration of monovalent ions lead to inhomogeneities in the NLO response of the poled zone.

In conclusion, we provide in this work a pathway to control and optimize the thermal field-assisted exchange of silver with sodium ions in sodium niobium borophosphate glasses. This was achieved by 1 h treatment at 230 °C under 1 kV. The resulting ions profile under the anode surface confirms that the introduction of silver is achieved with ions piled up behind the sodium depletion front. A quantitative SHG study of the poled glasses indicates also that the nonlinearity is confined in a layer of 4 μm with $\chi^{(2)} = \sim 1$ pm/V at the anode side. The accumulation of silver ions inside the depleted zone evidenced by EDS measurements is responsible for the decrease in the global signal from ~ 2 pm/V for BPN45 (Ref. 4) to ~ 1 pm/V for BPN45/Ag. This is confirmed by the THG measurements in the poled zone, which show that $\chi^{(3)}$ remains the same in both poled BPN45 and BPN45/Ag glasses. The decrease in the induced $\chi^{(2)}$ in BPN45/Ag is then unambiguously due to the modification of the embedded field in correlation with cations profiles in the poled regions.³

The NLO efficiency of this glass composition and the original nonlinear layer, which has been elaborated by the field-assisted ion-exchange, allows to be optimistic with their potential for future electro-optical applications, for example, the development of nonlinear waveguides.

ACKNOWLEDGMENTS

We acknowledge Région Aquitaine and the Agence Nationale de la Recherche (ANR) (Grant No. ANR-05-BLAN-0212-01) for financial support. A.M. is indebted to INTAS and RFBR under Grant No. 07-03-00573a for financial support.

¹R. A. Myers, N. Mukherjee, and S. R. J. Brueck, *Opt. Lett.* **16**, 1732 (1991).

²N. Mukherjee, R. A. Myers, and S. R. J. Brueck, *J. Opt. Soc. Am. B* **11**, 665 (1994).

³M. Dussauze, E. Fargin, M. Lahaye, V. Rodriguez, and F. Adamietz, *Opt. Express* **13**, 4064 (2005).

⁴M. Dussauze, E. Fargin, A. Malakho, V. Rodriguez, T. Buffeteau, and F. Adamietz, *Opt. Mater. (Amsterdam, Neth.)* **28**, 1417 (2006).

⁵M. Qiu, R. Vilaseca, C. Cojocar, J. Martorell, and T. Mizunami, *J. Appl. Phys.* **88**, 4666 (2000).

⁶V. Rodriguez and C. Sourisseau, *J. Opt. Soc. Am. B* **19**, 2650 (2002).

⁷A. Brocas, L. Canioni, and L. Sarger, *Opt. Express* **12**, 2317 (2004).

⁸T. Cardinal, E. Fargin, G. Le Flem, and S. Leboiteux, *J. Non-Cryst. Solids* **222**, 228 (1997).

⁹A. A. Lipovskii, D. K. Tagantsev, A. A. Vetrov, and O. V. Yanush, *Opt. Mater. (Amsterdam, Neth.)* **21**, 749 (2003).

¹⁰M. Dussauze, E. Fargin, V. Rodriguez, A. Malakho, and E. Kamitsos, *J. Appl. Phys.* **101**, 083532 (2007).

¹¹J. L. Barton, *J. Non-Cryst. Solids* **4**, 220 (1970).

¹²A. A. Lipovskii and V. V. Zhurikhina, *J. Non-Cryst. Solids* **351**, 3784 (2005).

¹³M. Dussauze, O. Bidault, E. Fargin, M. Maglione, and V. Rodriguez, *J. Appl. Phys.* **100**, 034905 (2006).

¹⁴A. Royon, B. Bousquet, L. Canioni, M. Treguer, T. Cardinal, E. Fargin, D. G. Kim, and S. H. Park, *J. Opt. Soc. Korea* **10**, 188 (2006).